Development of a Soot Radiation Model for Diesel flames

Authors:

J.J. López, J.M. García-Oliver, Antonio García, David Villalta

Affiliation:

CMT Motores Térmicos – Universitat Politècnica de València, Camino de Vera s/n, 46022, Valencia, Spain.

Corresponding Author:

Dr. Antonio García

CMT - Motores Térmicos /Universitat Politècnica de València

angarma8@mot.upv.es

HIGHLIGHTS

- Radiation model is based on two sub-models: spray model and soot model.
- The spray model estimates a penetration very similar to the experimental values.
- Soot Yield concept combines the soot formation and oxidation processes.
- Higher radiant fraction value is obtained when the oxygen molar fraction is reduced.
- The radiant fraction shows values from 0.11% to 0.43% respect to the total fuel energy.

KEYWORDS

Radiation; soot; heat transfer; spectral intensity; soot radiation model

ABSTRACT

This paper describes a radiation model for diesel sprays that can predict the heat losses based on spray characteristics to the spray plume due to radiation. The model is based on three sub-models: spray model, soot model and radiation model. The spray model is a one-dimensional model that simulates the axial and radial distribution of a fuel spray for each instant. The soot model is a one-dimensional tool, which is based on formation and oxidation processes calculating the axial and radial soot concentration profile for each instant. The output results of the two sub-models are used as input information for the radiation model, which obtains the radiation heat transfer values for a diesel flame. The experimental measurements used to adjust the different constants and to validate the sub-models were performed in a high-pressure high-temperature vessel using three different optical techniques: Schlieren, to obtain spray penetration, Diffused Back-Illumination technique (DBI) for the soot concentration and the 2-color method for calculating the soot temperature and concentration. The radiant fraction shows values from 0.11% to 0.43% with respect to the total energy of the fuel depending on the operating condition. Taking

into account the different assumptions taken for modeling the spray radiation, these results are consistent with those obtained in the literature, in which the radiation was characterized under similar conditions.

1. INTRODUCTION

Radiation heat transfer plays an important role in the heat transfer in direct-injection (DI) diesel engines, being a significant component of the efficiency losses in modern designs. Rough estimates of the heat transfer in the combustion chamber for the whole engine cycle show that radiation varies from 0.5-1 % [1] up to 5-10 % [2] of the total fuel energy depending on soot conditions (concentration and temperature). This value differs significantly depending on the geometry of the combustion chamber, fuel used, operating conditions, etc.

The main source of thermal radiation are soot particles, which emit radiation over the entire wavelength spectrum. It is worthy to note that radiation is also emitted by CO2 and H2O molecules but it is concentrate in a narrow spectral bands and its magnitude is assumed to be much smaller than that of soot particles [3]. Soot formation is a complex process comprising several physical and chemical phenomena, some of which occur simultaneously, and depends largely on local conditions. Computational models typically include processes such as precursor formation, particle inception, surface growth and particle oxidation. These models have typically been developed for use with CFD diesel engine models, but with a lower simulation cost. Regarding its use, soot emissions have been analyzed in different studies: for varying the injection timing [4], different oxygen concentrations in the intake air [5], adding post injection event [6] , etc. Deep knowledge of the processes that include soot particles is important for two main reasons: on the one

hand, soot emissions are limited by strict pollutant regulations. On the other hand, soot particles are mainly responsible for the total radiation heat transfer in diesel engines [7].

The main objective of this investigation is to develop a soot radiation model that it is able to predict the radiation heat losses. This study is based on the distribution of soot inside the flame, as well as understanding the processes that affect the radiation heat losses. For that, three sub-models have been used: spray model, which includes all the fundamental knowledge about combusting diesel sprays, a soot model, including both the formation and oxidation processes, and a radiation model. The radiation model simulates the temporal evolution of the spectral intensity, and consequently, the total soot radiation losses from the simulated soot concentration results.

2. EXPERIMETAL DATABASE

Throughout this study, experimental results previously published in [8] have been used to calibrate the different constants for each model. Post-processing has been adapted to compare with the simulated results in the different models. Next, the experimental facility used for the experimental measurements and the test conditions are described.

2.1. Experimental set-up: High pressure and high temperature vessel

The high pressure and high temperature (HPHT) vessel is an experimental facility, that allows to replicate engine like thermodynamic conditions to a diesel engine at the instant of injection (Figure 1). The vessel is classified as a constant-pressure flow (CPF) facility [9] as the conditions are reached by a continuous flow of high-pressure high temperature gas through the vessel. The vessel is equipped with three large optical accesses (128 mm in diameter) arranged in an orthogonal manner so that there is a full vision of the spray plume. The mechanical limits of the vessel are 15 MPa of gas pressure and 1000 K of gas temperature, and it is possible to obtain nearly quiescent and steady thermodynamic

conditions in the vessel. A common rail injection system allows changing the fuel injection pressure and the duration of injection.

Figure 1. High pressure and high temperature vessel [9]

The pressurized gas is supplied to the vessel by two volumetric compressors working in parallel, providing a continuous feed of 70 Nm^3/h. The vessel can work in open or closed loop to test spray evolution either in a standard air atmosphere or in gas mixtures with different O_2 concentrations.

To heat the air, two electrical heaters of 15 kW each are placed upstream the vessel. A secondary 2.5 kW heater is placed at the bottom of the chamber to help maintain the temperature. Additionally, a 3 kW heating liner is placed in the periphery of the vessel to minimize the heat losses from the ambient air.

2.2. Previous experimental results

The test matrix is conformed of six operating conditions from a previous study [8]. These operating conditions are based on ECN-Spray A reference conditions, using n-dodecane as fuel. The injection pressure was swept (500, 1000 and 1500 bar) as well as the O_2 molar fraction (15 and 21%) keeping the density constant at 22.8 kg/m^3 and the bulk gas temperature at 900 K.

Temperature [K]	Density [kg/m^3]	Injection pressure [bar]	Molar fraction O_2 [%]
900	22.8	500 / 1000 / 1500	15 / 21

Table 1. Operating conditions

A single-hole piezoelectric injector was used with a nominal diameter nozzle of 90 μm. The energizing time (ET) of the injector was set at 2 ms for all conditions, which results in a 3.5 ms hydraulic duration. Each measurement consisted on 10 repetitions in order to reduce the experimental measurement uncertainties.

The operating conditions were measured by three different optical techniques:

- Schileren optical technique [10]: a conventional Schlieren single-pass arrangement was employed to detect the complete spray boundaries at high temperature and high pressure conditions. Schlieren imaging technique enables to detect gradients in the refractive index of a transparent medium. The technique relies on the deviation of a light beam produced when light passes through non-homogeneous fluids. For this study, this optical technique has been used to obtain spray penetration.
- Diffused Back-Illumination technique (DBI) [11]: as an extinction-based diagnostic, the soot volume fraction is related to the amount of light that has been absorbed or scattered by the soot cloud. For this work, the temporal and spatial soot concentration (KL) are obtained by DBI technique to compare with the modelled soot concentration results.
- 2-color method (2C) [12]: it is an optical thermometry technique that makes use of the presence of soot within a flame. It is particularly useful for diesel combustion studies due to the fact that soot incandescence dominates the flame radiation emission during most of the heat release period. In this sense, flame images recorded by means of conventional visualization techniques in the visible

spectrum are basically soot radiation images. In this work, the 2-color method was used to calculate the soot temperature and concentration.

3. METHODOLOGY

The structure of the complete radiation model is shown in Figure 2. Three sub-models, which are directly connected to each other, compose the whole model. The spray model (named DICOM) is a one-dimensional model that simulates the axial and radial distribution of a fuel spray for each instant. This model needs input variables such as the temporal evolution of the ambient pressure, ambient density, injection rate and the spray angle that is necessary to calibrate with experimental data. For this, the experimental results of spray penetration in both inert and reactive environment measured with the Schlieren technique will be used to adjust the spray angle parameter (Section 4.3).

Once the spray model has been calibrated, these spray model results have been used as input variables for the soot model and thus, axial and radial profiles of soot mass fraction have been obtained for each instant. As in the spray model, in the soot model the optimal values for two constants (K_{soot} and T_0) need to be adjusted from experimental results of soot concentration (Section 5.2). These experimental results have been measured with the Diffused Back-Illumination technique (DBI). In the next step, the temporal evolution of the spectral intensity has been obtained from the simulated soot concentration results together with the spatial temperature distribution calculated also in the spray model (Section 6.3). Finally, the simulated spectral intensity is integrated for the whole wavelengths spectrum and the radiation heat losses are obtained. As in two previous models, the simulated radiation has been compared with experimental values from the 2-Color method.

154 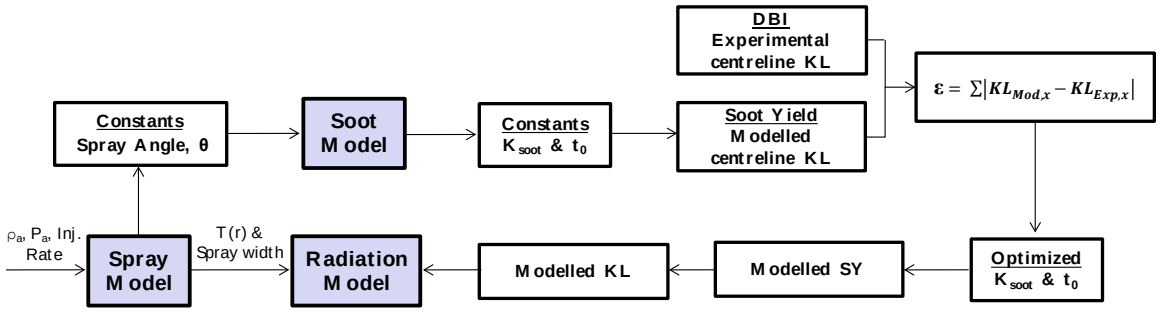

155 *Figure 2. Overall model structure*

156 # 4. SPRAY MODEL

157 Currently, there are several computational models capable of analyze and characterize the
158 internal diesel spray structure in an injection/combustion process with temporal and
159 spatial resolution. The set of computational tools ranges from complex models (known as
160 3D CFD) to more simplified models in which certain assumptions are made. In this work
161 a one-dimensional model has been selected, which adapts perfectly to requirements of the
162 analysis and has a short calculation time.

163 ## 4.1. Spray model description

164 The spray model is a one-dimensional model capable of simulating the temporal and
165 radial evolution of a fuel spray for inert (evaporative or non-evaporative) and reactive
166 conditions, as well as for steady and transient conditions. This model has been developed
167 by the CMT - Motores Térmicos group of the Universidad Politécnica de Valencia. This
168 model is described in more detail in previous works [13][14].

169 The model approaches the analysis of a fuel spray injected through a single hole inside a
170 closed volume, where the process of air/fuel mixing and the combustion processes are
171 reproduced. The spray evolution is considered free of any spatial restriction and the closed
172 volume is considered wide enough so that the air conditions remain constant.

The model requires certain experimental data such as the temporal evolution of the ambient pressure, the ambient density and the injection rate, injector properties (orifice number, diameter, spray angle) and fuel. As output values, the model generates comprehensive results, which describe the air/fuel mixture process with axial and temporal resolution. These results are used as input values in the soot and radiation models.

4.2. Spray model calibration under inert conditions. Spray Angle

As mentioned in section 3, the only unknown input of the model is the spray angle; therefore, it needs to be determined by adjusting the results of the modelled vapor penetration to the experimental Spray-A results, defined in table 1.

To validate the model and to determine the adequate spray angle for a given set of conditions, a series of calculations were made at small angle increments (1°); then, the deviation from the experimental curves was determined, and based on that, the value for the angle was chosen. Figure 3 shows the experimental vapor penetration for the Spray-A standard conditions and the curves for three different spray angles as predicted by the model. It can be seen that a wider angle (24°) tends to under-predict the penetration, while a narrower angle (22º) may seem more appropriate at the beginning of the spray, but at the end, it overestimates the penetration values with respect to the experimental case. In this case, the best match between experimental and simulation data was achieved at spray angle of 23º.

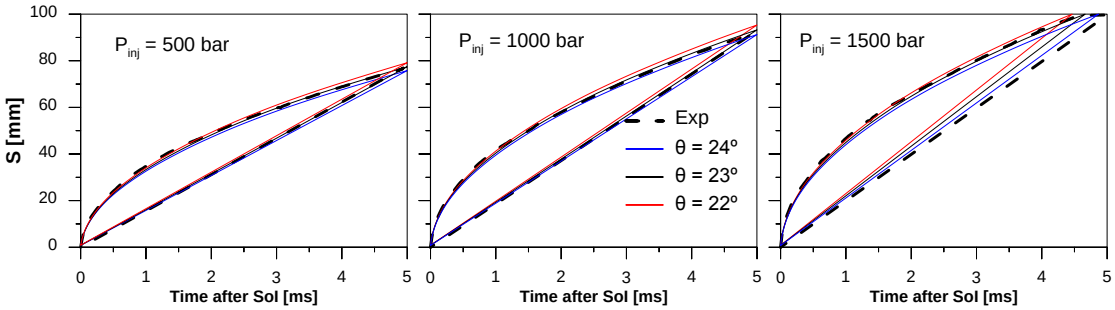

194

195 *Figure 3. Experimental and modelled vapor penetration for the three spray angles and different injection*
196 *pressures tested under inert conditions*

197 Figure 4 shows the temporal evolution of the difference (in absolute values) between the
198 experimental and modelled vapor penetration for the three spray angles tested and for the
199 three different injection pressures. In addition, it has been found in the literature [15][16]
200 that the spray angle depends mainly on ambient density and the injection pressure. In this
201 investigation only the injection pressure has been varied. Although there are differences
202 depending on the injection pressure, they are small to choose a different spray angle
203 depending on the injection pressure. Therefore, the angle selected was 23° since it
204 presented a good balance between the near and far regions of the spray from the nozzle.

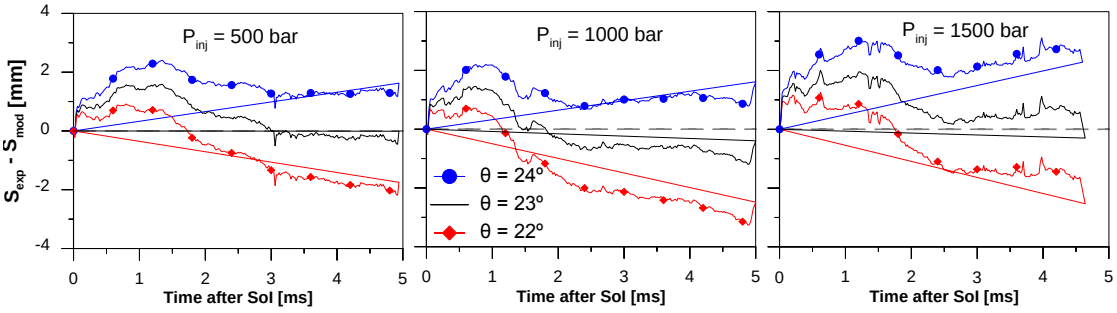

205

206 *Figure 4. Difference between experimental and modelled vapor penetration for the three spray angles*
207 *and different injection pressures tested under reactive conditions*

208

209 **4.3. Spray model validation under reacting conditions**

210 To determine the most suitable angle for the operating conditions measured, the model
211 has calculated the vapor penetration under reactive conditions with the selected angle in

inert conditions (23°). The results obtained have been compared with the experimental values for determining the most adequate spray angle.

Prior to the comparison, it is necessary to describe the methodology used to obtain the experimental spray penetration from the images. The technique used to obtain spray penetration was Diffused Back-Illumination technique (DBI). Each image corresponds to a spatial distribution of the DBI signal (KL) every 100 μs. The DBI signal distribution is shown at the top image of Figure 5. To acquire the spray penetration, the DBI signal values along the central axis have been plotted (bottom image of Figure 5), taking as center line, an imaginary axis that comes from the center of the nozzle. For each image, the furthest location on the axis where the DBI signal exceeds a threshold is defined as the flame penetration. In this way, a temporal evolution of the flame penetration is represented from the experimental images.

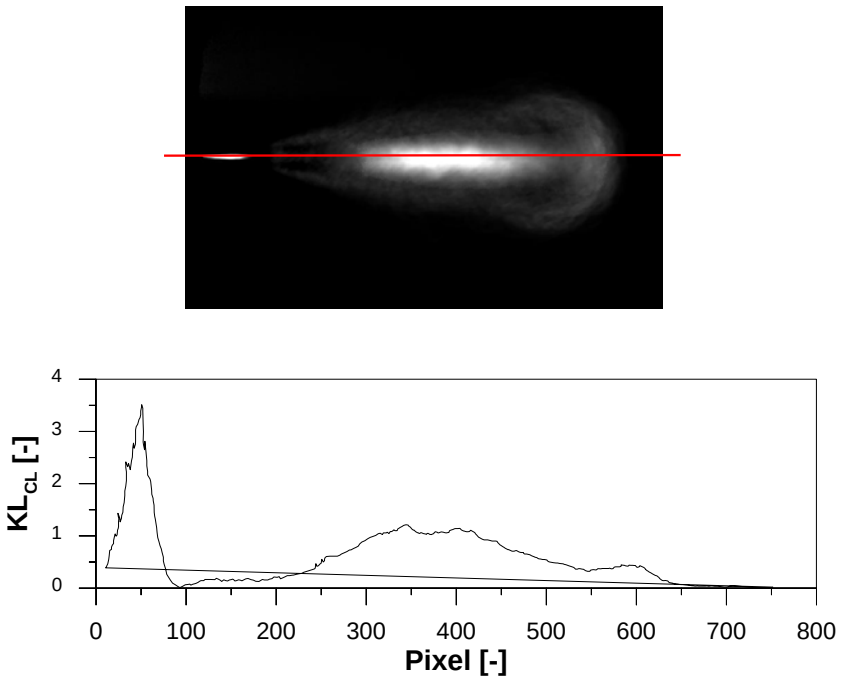

Figure 5. Top) Spray image obtained from the Diffused Back-Illumination technique and bottom) the soot concentration profile in the centerline.

Figure 6 shows the temporal evolution of the experimental spray penetration (solid line) and modelled (dashed line) for the six operating conditions analyzed. It should be noted

that there is a field of view limitation caused by the optical access of the vessel. Therefore, the maximum penetration able to be captured in the experimental measurements was 86 mm. As shown in Figure 6, the temporal evolution of the flame penetration is split in two stages. First, one is the transient stage, in which the flame penetration increases progressively, where the modelled and experimental results show small differences (at least until the distance of 86 mm).The second is the steady stage where the flame penetration maintains a quasi-constant value (the flame front is stabilized). This phase can only be observed in 21% oxygen results due to the above-mentioned limitation in optical access. For lower oxygen concentration, stabilized flame penetration extends to approximately 110 mm [17]. The flame penetration in the steady zone presents slight differences (around 5 mm), which is due to a deviation from the acceptable experimental values. Thus it is possible to conclude that, at least for the whole conditions used in this study, the most suitable spray angle is 23°.

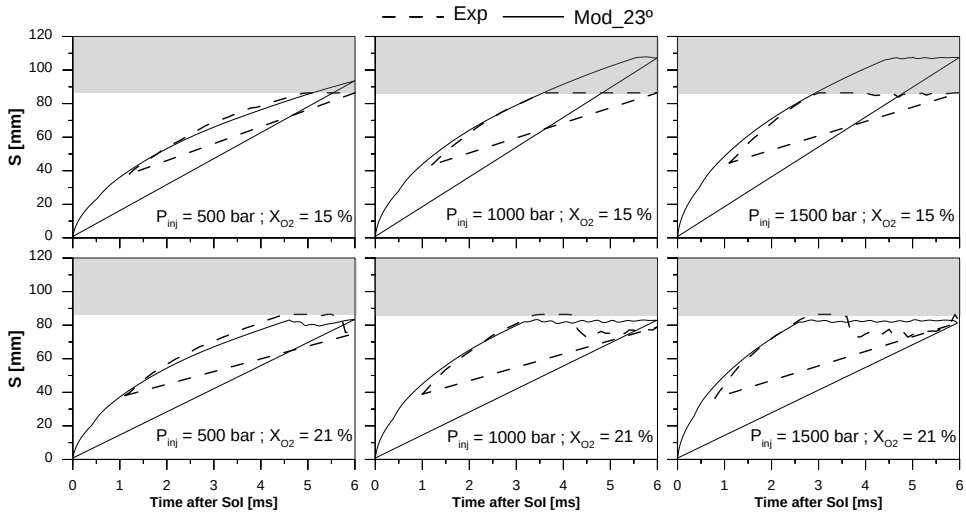

Figure 6. Experimental and modelled spray penetration under reactive conditions for the six conditions tested.

5. SOOT MODEL

In this section a one-dimensional soot model is presented. This model considers both soot formation and oxidation processes. The model uses the calculated results in the one-dimensional spray model as input variables, thus obtaining axial and radial soot concentration profiles for each instant in a diesel flame. In a first section, the model will be described along with the equations. Then, the necessary constants will be adjusted from the experimental results. Finally, the model will be validated with experimental data.

5.1.Soot model description

The soot model is based on Monin's study [19]. In this work, a parameter was proposed to model the soot formation process easily. The parameter was referred to as “soot yield” (SY) and is defined as the ratio between the mass fraction of fuel transformed into soot (Y_{soot}) and the mass fraction of unburned available fuel at that location (Y_{f_nb}):

(1) $$SY = \frac{Y_{soot}}{Y_{f\_nb}}$$

It is important to define non-burned fuel mass fraction parameter for each instant and flame location. This mass includes all the mass coming from the unburned fuel that is available in that location with no distinction of its state (original fuel, cracked fuel, partly oxidized fuel or soot). This parameter is an input value to the soot model from the spray model (mixing/combustion).

Later, López et al. [20] proposed a correlation for the SY:

(2) $$SY = K_{soot} \cdot max\left(0.5 - \frac{1}{Fr_{LOL}}, 0\right) \cdot t_r \cdot exp\left(\frac{T_0}{T_{Flame}}\right) \cdot \rho^{2.2}$$

where Fr_{LOL} is the fuel-air equivalence ratio at the lift-off length, t_r is the residence time inside the flame, T_{Flame} is the flame temperature, ρ is the ambient density and K_{soot} and T_0 are constant and their values have been fitting from experimental values (section 5.2).

- As many other researchers have observed [5][21] the soot formation process is mainly controlled by the fuel-air equivalence ratio at the lift-off length. Usually, a fuel-air equivalence ratio (Fr_{LOL}) of 2 is the limit to define whether soot is produced (Fr_{LOL} higher than 2) or not (Fr_{LOL} lower than 2) in a combusting diesel spray. For this reason, the soot yield is assumed to be different from this value. Finally, the Fr_{LOL} is an input variable to the soot model calculated by the spray model (mixing/combustion).
- The soot formation also depends on the residence time of the fuel inside the fuel-rich region of the reacting spray. The residence time parameter is defined as $t-t_{LOL}$, where t is the instant under study and t_{LOL} stands for the time at which the considered fuel reaches the lift-off length. The SY is proportional to t_r. As it is well known, an increase in temperature at the lift-off length implies an improvement in soot formation. Monin [19] assumed that this parameter affects exponentially the rate of soot formation process: exp (T_0/T_{Flame}), where T_0 is a constant obtained from comparison with experimental results.
- Finally, Pickett found that the soot formation process is also affected by the ambient pressure (or, for a given temperature, by density) [21]. Based on the data published in his work, the corresponding function is the following: $\rho^{2.2}$, which also should affect the soot yield.

Once the factors, the SY parameter depends on, are defined from the product of equations (1) and (2) the mass fraction of soot, Y_{soot}, can be obtained. Nevertheless, both two and both most common soot measuring techniques (DBI and two-color method) provide a

value for X_{soot} (volume fraction). Consequently, the conversion from one magnitude to the other is required. This conversion can be done as follows:

$$X_{soot} = Y_{soot} \cdot \frac{\rho_a}{\rho_{soot}} \quad (3)$$

where ρ_{soot} is the density of the soot particles and ρ_a is the density at the point under consideration (local density). The soot particle density does not have a universal value. However, some authors take a value of approximately 1800 kg/m^3 as a representative value [22]. For the local density estimation, the local temperature and the mean pressure are considered, assuming standard air for the constant in the equation of state.

Up to now, the soot model is able to predict the evolution of X_{soot} at the spray centerline. As soot radiation takes place at any region where temperature is sufficiently high, the value of the soot volume fraction at any other point of the spray section is needed. There is not much information available in the literature about the shape of the X_{soot} radial profile. For this model, a Gaussian profile has been chosen to simulate the flame section, similar to mixture fraction profiles as in [24], which follows the following equation:

$$\frac{X_{soot}}{X_{soot,CL}} = exp\left[-4.6 \cdot \left(\frac{r}{R_{Flame}}\right)^2\right] \quad (4)$$

where r is the radial coordinate and R_{Flame} the flame radius at the section under consideration.

5.2. Adjustment methodology. Soot model validation

This section describes the calibration of the model constants, K_{soot} and T_0, and the soot model validation. For both objectives, experimental results of the soot concentration from the Diffused Back-Illumination technique (DBI) were used.

312 The flow chart in Figure 7 describes the methodology used to calibrate the constants K_{soot}
313 and T_0 is shown. These two parameters have been found by searching the lowest error
314 when comparing the experimental and the modelled soot concentration at each axial and
315 radial position. This procedure was divided into several steps:

316 • First, an initial value is assigned to each constant. With them, the parameter SY is
317 calculated. As described in section 5.1, a soot molar fraction value (X_{soot}) is
318 obtained for each flame axial and radial position. Next, the soot concentration
319 values (KL) is calculated from the information of the soot model and compared
320 with the experimental values provided by the DBI method. The conversion of X_{soot}
321 to KL is based on the Beer-Lambert equation, which evaluates the light
322 attenuation [18]:

323 (5) $$\frac{\boldsymbol{I}}{\boldsymbol{I_0}} = exp(-KL) = \tau$$

324 where I_0 is the incident light intensity, I is the attenuated light intensity and τ, the
325 transmissivity. If it is considered that the flame is divided radially into n elements
326 with the same thickness, the equation (5) can be rewritten as follows:

327 (6) $$\frac{\boldsymbol{I}}{\boldsymbol{I_0}} = exp(-KL) = \tau = \sum_{i=1}^{n} \tau_i$$

328 where τ_i represents the transmissivity of each portion of the spray. According to
329 Musculus [18], the transmissivity is related to the soot volume fraction in the
330 following way:

331 (7) $$\tau_i = exp\left(\frac{-g \cdot X_{soot(r) \cdot dr}}{\lambda^{\alpha}}\right)$$

332 where g is a constant equal to 6.3 μm^{-1}, λ is the wavelength in μm and α = 1.22-
333 0.245·ln (λ), with λ in μm and dr is the thickness for each element. If equations

(6) and (7) are considered together, and it is taken into account that the product of an exponential is the exponential of an addition, it can be seen that KL can be related to the local conditions in the following way:

$$KL = \frac{g}{\lambda^{\alpha}} \cdot \int_{-L/2}^{+L/2} X_{soot}(r) \cdot dr \quad (8)$$

To finish this first step, the difference (ε) of the modelled and experimental soot concentrations for each axial and radial position is calculated.

- The second stage consists of performing the same previous procedure until reaching the sum of the differences, but in this case varying the values of both constants. In particular, both constants were varied ± 20% of their initial value. This indicates that the first step is repeated with all possible combinations of the constants, that is, four times.
- Finally, the constant combination with lower value is chosen from the five error results (initial + 4 combinations). This pair of constants are considered as initial values and the whole procedure is repeated, so that finally a matrix with five accumulated errors corresponding to five constant pairs is obtained again. This step is repeated until the minimum error is achieved twice times consecutively by the same constants K_{soot} and T_0.

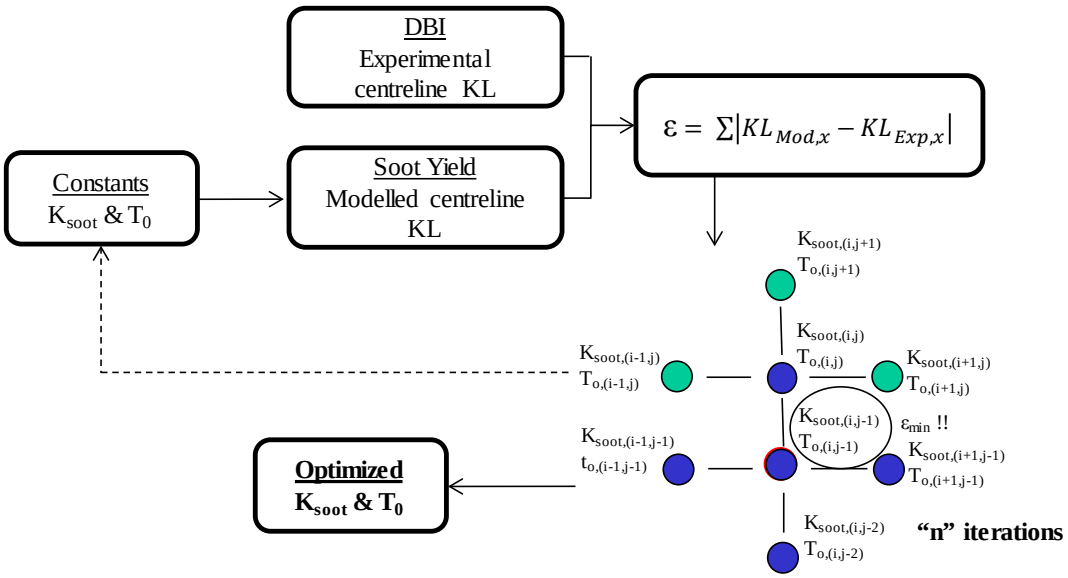

Figure 7. Experimental methodology used to fit/adjust the soot model constants (K_{soot} and T_0).

Considering the six operating conditions described in the test plan section, the values obtained for the constants K_{soot} and T_0 are $11.25 \cdot 10^{-4}$ and 4687.5 K, respectively. Figure 8 shows the axial evolution of the experimental and modelled soot concentration along the flame centerline at a given instant. The model adjusts the start and end of the flame precisely. Qualitatively, the modelled results show good agreement with experimental data (KL decreases when the injection pressure increases and/or the oxygen concentration increases). Therefore, it is concluded that the soot model is correctly calibrated respect to the experimental data.

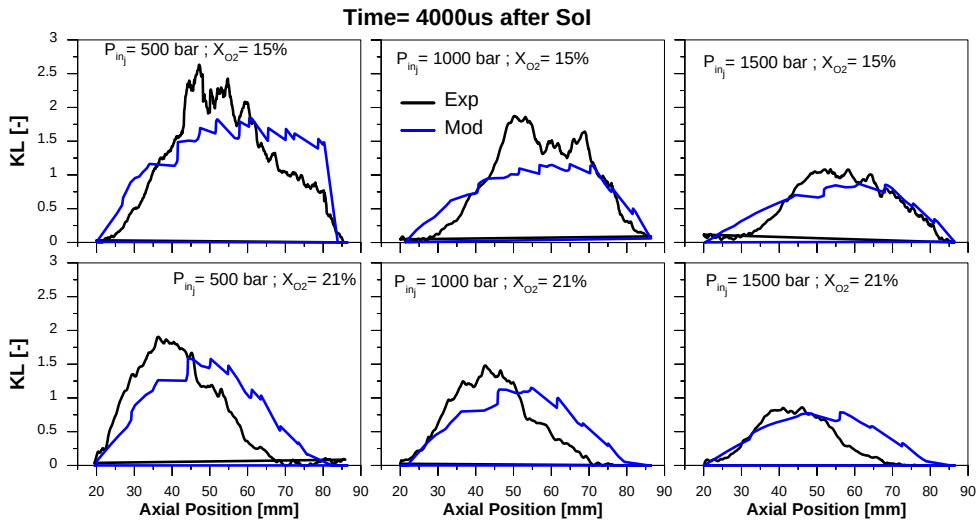

Figure 8. Experimental and modelled soot concentration for six operating conditions.

6. RADIATION MODEL

This section presents the radiation model and the methodology to validate the model. For that, the spectral intensity of the radiation (I_{soot}) has been calculated and compared to the experimental values measured by the 2-color method. Then, the total radiation emitted by the soot is calculated.

To begin with, these are the different assumptions taken for modeling the spray radiation:

- The spray/wall interaction will not be considered. Consequently, a free spray is considered.
- The swirl existing in the combustion chamber does not modify the spray geometry, which remains axisymmetric.
- The radiation is diffuse and it radiates in the same way in all directions.

6.1. Model description

The radiation intensity is the main output variable of the radiation model (as shown in Figure 2) and this has been used as a basis to validate the present radiation model. The

radiation intensity in the radial direction has been calculated as explained by Payri *et al.*[25].

Figure 9 presents the modelled combustion temperature and soot distribution for a particular axial position. The temperature distribution has been obtained from the spray model, as a function of the equivalence ratio distribution at each radial and axial position. Three different zones can be observed in the temperature distribution: 1) the flame limits are the stoichiometric surface, where the maximum temperatures are reached; in this location the fuel diffused from the inner part of the flame reacts with oxygen from the outer part. 2) the inner zone, which corresponds to the rich side of the flame; this region consists of partially oxidized fuel, combustion products and soot. 3) the outer part, which is the lean side of the flame; in this region fresh air and combustion products are present. In terms of soot concentration, a linear distribution has been considered in which it is assumed that the soot particles are only present in the inner part of the flame, as they are totally oxidized by the OH present on the reaction zone [26].

The flame is divided radially into discrete flame elements with their corresponding values of temperature and soot concentration. To analyze the radiation propagation inside the flame, both emission and absorption processes have been considered.

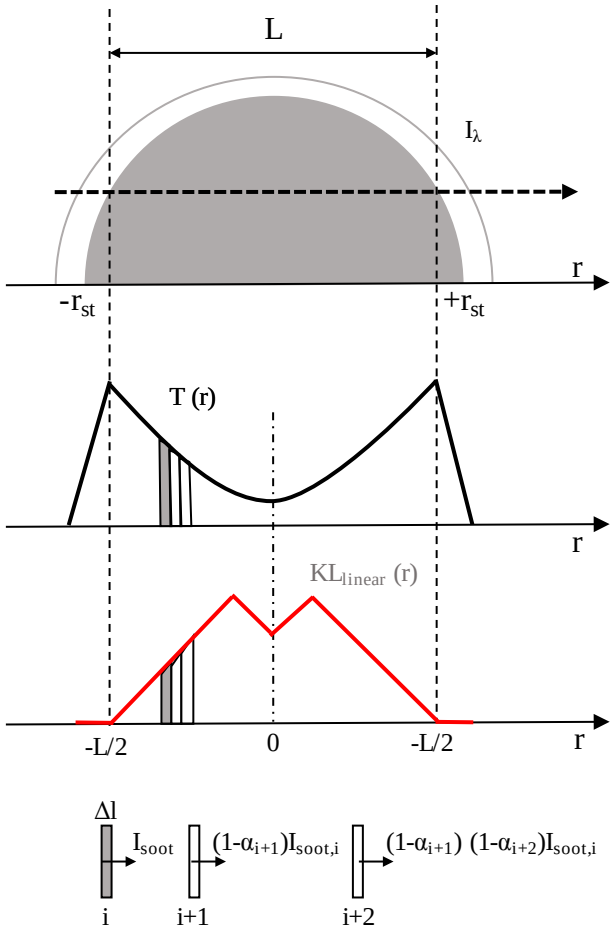

Figure 9. Scheme radiation propagation through of the diesel spray [25]

Considering the temperature and soot distributions, the radiation propagation process inside the flame is based on the following:

- Radiation is propagated along lines parallel to the flame main symmetry plane.
- The spatial distribution of the local gas temperature is assumed to be equal to the soot temperature. In this case, the spray model calculates the flame temperature.
- Soot is assumed to be completely oxidized at the flame stoichiometric surface.

The radiation path is divided into *n* elements with the same thickness. Each element *i* has its temperature T_i and optical thickness KL_i. So, considering the proposed soot distributions it can be stated that:

406 *(9)* $$KL = \sum_{i=1}^{n} (KL)_i$$

407 As indicated in the description of the 2-color method [12], the radiation emitted by each
408 element can be calculated as:

409 *(10)* $$I_{soot,i}(\lambda, T_i, KL_i) = \varepsilon_{\lambda,i} I_{b(\lambda,T_i)}$$

410 where ε indicates soot spectral emissivity and I_b corresponds to a blackbody spectral
411 intensity. The radiation received by the sensor (which is located on either flame limits) at
412 each wavelength is the addition of the $I_{soot,i}$ of each flame element. Considering the
413 attenuation factor between elements, the total soot radiation intensity for each wavelength
414 can be calculated as:

415 *(11)* $$I_{soot,i}(\lambda, T_i, KL_i) = \sum_{i=1}^{n} \left[\varepsilon_{\lambda,i} I_{b(\lambda,T_i)} \cdot \prod_{j=i+1}^{n} (1 - \alpha_{\lambda,j}) \right]$$

416 where for an element *j* the absorption ($\alpha_{\lambda,j}$) is defined by the spectral absorptivity ($\varepsilon_{\lambda,j}$)
417 as stated by Kirchhoff's law:

418 *(12)* $$\alpha_{\lambda,j} = \varepsilon_{\lambda,j}$$

419

420 **6.2. Spectral intensity**

421 The purpose of this section is to evaluate the soot spectral intensity (as an output
422 parameter of the radiation model) versus the experimental results from the 2-color
423 method.

424 Figure 10 shows the axial evolution of the experimental and modelled soot spectral
425 intensity along the centerline for the six operating conditions. The soot spectral intensity
426 has been calculated for two wavelengths, λ = 550 and 650 nm. For simplicity, only the
427 results for λ = 550 nm are shown. In general, both modelled and experimental soot
428 spectral intensity values decrease when the injection pressure increases and/or the oxygen

mass fraction increases. By comparing each graph individually, it can be established that the model provides a good accuracy during the onset of the flame. If the flame length is divided into two parts, in the first one, the model sub-predicts the soot spectral intensity values. This phase is estimated up to 60-70 mm from the injector. From this, the trend changes and the model over-predicts the results respect to the experimental results.

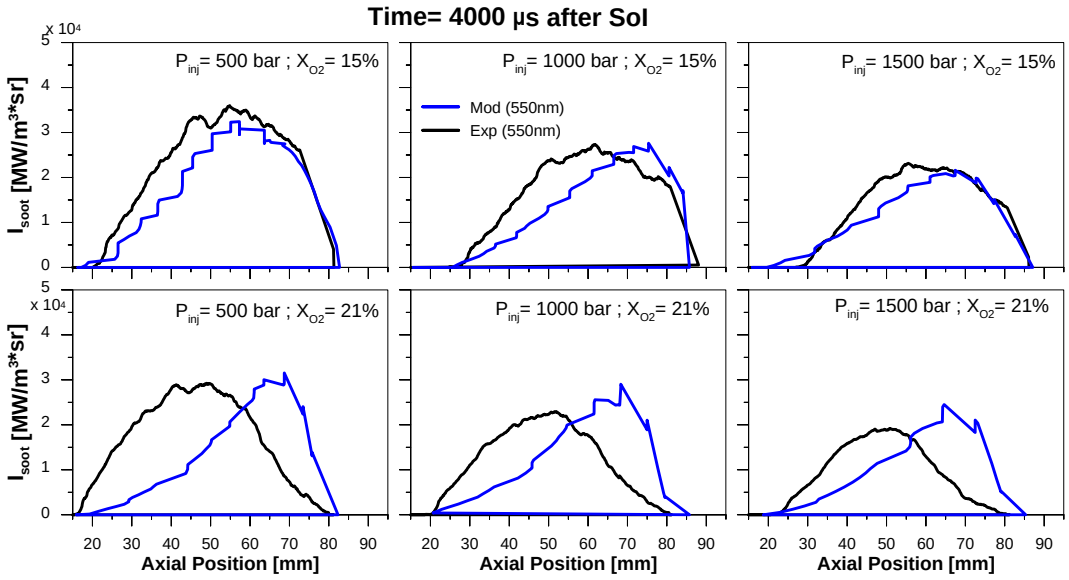

Figure 10. Experimental and modelled soot spectral intensity along the spray centerline for the six operating conditions.

6.3. Total radiation

The next step in the validation of the radiation model is the calculation of the total radiation emitted by soot particles. Based on the soot spectral intensity, the total radiation was obtained from the integration of the spectral intensity for a particular range of wavelengths using equation (13):

$$Q_{rad} = \pi \int_t \int_A \int_\lambda \varepsilon_\lambda I_{b,\lambda} \, d\lambda \, dA \, dt \qquad (13)$$

where t represents the exposure time in which the optical system is registering flame luminosity, and A is the flame area obtained by equation (14):

445 *(14)* $$A_t = 2\pi r \int_x dx$$

446 where *r* is the flame radius, which is determined from a temporal image of the flame, and
447 *dx* is the axial width.

448 Figure 11 represents the temporal evolution of the experimental and modelled total
449 radiation for the six operating conditions studied. For the six cases analyzed, the model
450 predicts total radiation values similar to the experimental. Considering the simplifications
451 and assumptions of each model, the results shown in Figure 11 can be considered as
452 acceptable results.

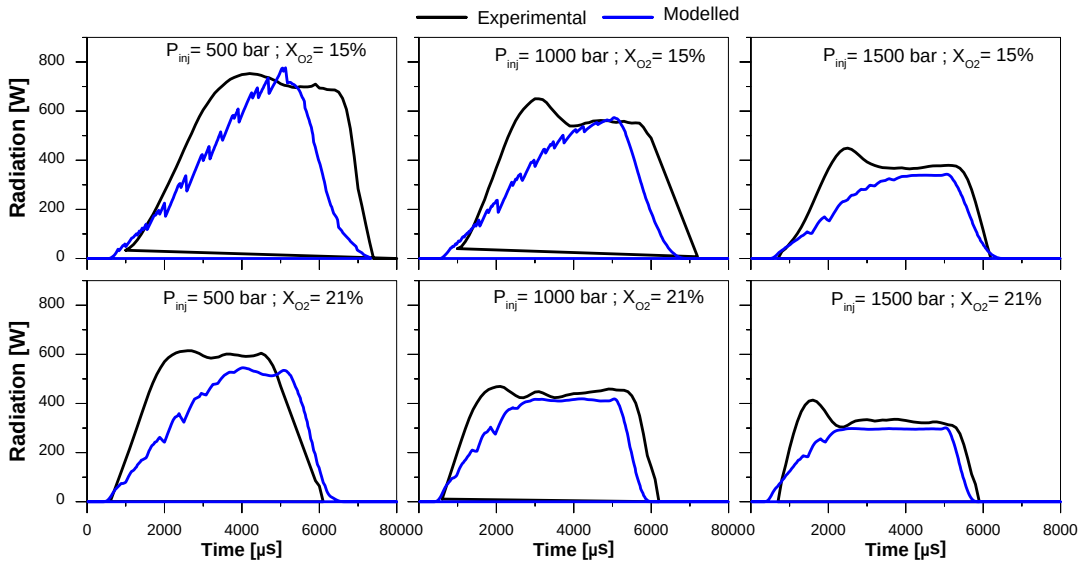

453

454 *Figure 11. The temporal evolution of the experimental and modelled total radiation for the six operating*
455 *conditions studied.*

456 Finally, to better quantify the total radiation, the radiant fraction has been calculated. The
457 radiant fraction (X_{rad}) emitted by soot is defined as the fraction of the total chemical
458 energy released during injection that is lost due to radiation heat transfer. This term is
459 expressed by equation (15):

460 *(15)* $$X_{rad} = {Q_{rad}}/{m_f Q_{LHV}}$$

where m_f represents the mass of fuel injected and Q_{LHV} is the lower heating value of dodecane (44.2 MJ/kg).

Figure 12 shows the results of the radiant fraction emitted by soot for the different operating conditions analyzed. Particularly, the sub-figure on the left shows the values of radiant fraction modifying the injection pressure at oxygen molar fraction of 15% and, the figure on the right, at oxygen molar fraction of 21%. Considering the results obtained from soot concentration and spectral intensity in previous figures, the trends of radiant fraction are expected. Thus, a reduction of injection pressure and/or oxygen molar fraction implies a higher radiant fraction value. In addition, as in the previous graph of the total radiation, the modelled radiant fraction values are slightly lower than the experimental ones. Finally, the modelled radiant fraction values are between 0.11 and 0.43% respect to the total fuel energy. Comparing them with the results obtained from the radiant fraction in [5], the modelled values are in the same order of magnitude. Considering that the operating conditions are similar, the modelled results are coherent with those obtained in [5]. This makes the radiation model a completely suitable tool to predict and study the radiation heat transfer.

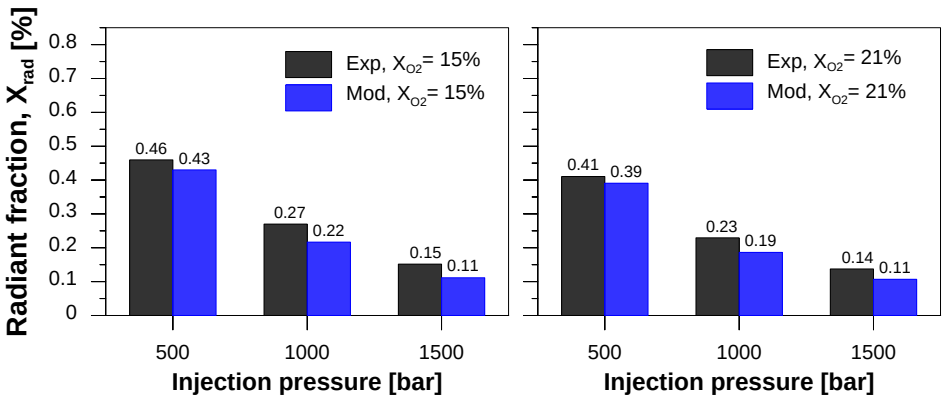

Figure 12. Experimental and modelled radiant fraction modifying injection pressure and oxygen molar fraction.

7. CONCLUSION

In this study, a radiation model for diesel spray has been developed. This model is able to predict the radiation from spray plume. The model is based on three sub-models: a spray model, which analyzes and characterizes the internal spray structure in terms of mixing and combustion process with temporal and spatial resolution. A soot model, based on soot formation and oxidation processes. The cohesion of these two sub-models is used to obtain the input values to the third model, the radiation model from which the radiation heat transfer values for a diesel flame are obtained. The main contributions of this paper are:

- The one-dimensional spray model has been adjusted for the only unknown variable: the spray angle. For the cases analyzed here, the most suitable spray angle has been found to be 23° comparing the penetration results in inert conditions. Regarding the validation of the model, penetration values have been used in reactive conditions. The model estimates a penetration very similar to the experimental values, both in the transient and quasi-steady phases.
- The soot model is based mainly on the "soot yield" concept, which combines the soot formation and oxidation processes depending on the time and location. This model has been calibrated by means of two unknown constants: K_{soot} and T_0. The values of the constants are $11.25 \cdot 10^{-4}$ and 4687.5 K, respectively. These constants have been obtained from an experimental methodology, where the soot concentrations are compared with the experimental values measured by Diffused Back-Illumination technique (DBI). The model predicts accurately the start and end of the flame. Although in qualitative terms, the model accurately predicts the experimental values. Depending on the axial position, the model sub-predicts or

over-predicts the experimental values. In general terms, the soot model matches correctly with the experimental values.

- Finally, a methodology developed by Payri was used for the radiation model [25]. The methodology has considered both emission and absorption processes for analyzing the radiation heat transfer inside the flame. From the soot concentration estimated with the soot model and the soot temperature calculated from the spray model, the modelled spectral intensity has been calculated. For the operating conditions used in this study, the radiation model calculates radiant spectral intensity values very similar to the experimental ones. Considering the simplifications and assumptions of each model, it can be accepted as acceptable results. The fraction of radiation shows values from 0.11% to 0.43% respect to the total fuel energy depending on the operating condition. Considering the differences in the operating conditions, these results are consistent with those obtained in [5], in which the radiation was characterized under simplified conditions. It is interesting to note that to determine the fraction of radiation, it is only necessary to have the temporal evolution of the ambient pressure, the ambient density and the injection rate, injector properties (orifice number, diameter, spray angle) and properties of the fuel in addition to the boundary conditions in which the operating conditions are tested. These experimental data can be obtained quite easily.

ACKNOWLEDGMENTS

The authors acknowledge FEDER and Spanish Ministerio de Economía y Competitividad for partially supporting this research through TRANCO project (TRA2017-87694-R).

REFERENCES

[1] P. Vogelin, Experimental investigation of multi-in-cylinder pyrometer measurements and exhaust soot emissions under steady and transient operation of a heavy-duty diesel engine, SAE technical paper 131ICE-0145; 2013.

[2] FJ. Struwe, In-cylinder measurement of particulate radiant heat transfer in a direct injection diesel engine, SAE technical paper 2003-01-0072; 2003.

[3] P. Furmanski, J. Banaszek, T. S. Wisniewski, Radiation Heat Tranfer In a Combustion Chamber of Diesel Engine with Partially Transparent Burnt Gas Zone. SAE Technical Paper 980504, 1988.

[4] D. Jung, D. Assanis, Multi-zone DI diesel spray combustion model for cycle simulation studies of engine performance and emissions, SAE paper 2001-01-1246; 2001.

[5] X. Bi, H. Liu, M. Huo, C. Shen, X. Qiao, C. F.Lee, Experimental and numerical study on soot formation and oxidation by using diesel fuel in constant volume chamber with various ambient oxygen concentrations, Energy Conversion and Management, Vol. 84, pp. 152-163, 2014.

[6] J. Benajes, J. Martín, A. García, D. Villalta, A.Warey, Swirl ratio and post injection strategies to improve late cycle diffusion combustion in a light-duty diesel engine, Applied Thermal Enginnering, Vol. 123, pp. 365-376, 2017.

[7] J. Benajes, J. Martín, A. García, D. Villalta, A.Warey, In-cylinder soot radiation heat transfer in direct-injection diesel engines, Energy Conversion nad Management 106, 414–427, 2015.

549 [8] S. Skeen, J. Manin, L. Pickett, E. Cenker et al., A Progress Review on Soot
550 Experiments and Modeling in the Engine Combustion Network (ECN), SAE Int. J.
551 Engines 9 (2), 2016.

552 [9] R. Payri, F.J. Salvador, P. Martí-Aldaraví, D. Vaquerizo, ECN Spray G external
553 spray visualization and spray collapse description through penetration and
554 morphology analysis, Applied Thermal Enginnering, Vol. 112, pp. 304-316, 2017.

555 [10] R. Payri, J.M. Garcia-Oliver, T. Xuan, M. Bardi, A study on diesel spray tip
556 penetration and radial expansion under reacting conditions, Applied Thermal
557 Enginnering, Vol. 90, pp. 691-629, 2015.

558 [11] J.V. Pastor, J.M. Garcia-Oliver, R. Novella, T. Xuan, Soot Quantification of Single-
559 Hole Diesel Sprays by Means of Extinction Imaging, SAE Int. J. Engines 8 (5),
560 2015.

561 [12] J. J. López, J. Martin, A. Garcia, D.Villalta, A. Warey, Implementation of two color
562 method to investigate late cycle soot oxidation process in a CI engine under low
563 load conditions, Applied Thermal Enginnering, Vol. 113, pp. 878-890, 2017.

564 [13] J. V. Pastor, J. J. Lopez, J. M Garcia-Oliver, J. M. Pastor, A 1D model for the
565 description of mixing-controlled inert diesel sprays, Fuel, Vol. 87 no 13-14, pp.
566 2871-2885, 2008.

567 [14] J.M. Desantes, J.V. Pastor, J.M. García-Oliver, J.M. Pastor, A 1D model for the
568 description of mixing-controlled reacting diesel sprays, Combustion and Flame,
569 Vol. 156, pp. 234-249, 2009.

570 [15] J.V. Pastor, J.M. Garcia-Oliver, J.M. Pastor, W. Vera-Tudela, One-dimensional
571 diesel spray modeling of multicomponent fuels, Atominzation and Sprays, Vol
572 25(2), pp. 485-517, 2015.

[16] E. Mancaruso, L. Sequino, B. Vaglieco, Analysis of spray injection in a light duty CR diesel engine supported by non-conventioanl measurements, Fuel Vol. 158, pp. 512-522, 2015.

[17] D. Siebers, B. Higgins, L. Pickett, Flame Lift-off on direct-injection diesel fuel jets: Oxygen concentration effects, SAE Technical Paper, nº 2002-01-0890, 2002.

[18] M. Musculus, Measurements of the Influence of Soot Radiation on In-Cylinder Temperatures and Exhaust NOx in a Heavy-Duty DI Diesel Engine, SAE Technical Paper, nº 2005-01-0925, 2005.

[19] C. Monin, Caracterización del Proceso de Formación de Hollín en una Llama de Difusión Diésel de Baja Temperatura, Doctoral Thesis, 2009.

[20] J. López, J.M. Garcia-Oliver, J. Martin, J.P. Chemisky, A. Bouet, A Soot Radiation Model for Diesel Sprays, SAE Technical Paper, nº 2012-01-1069, 2012.

[21] L.M. Pickett, D.L. Siebers, Soot in diesel fuel jets: effects of ambient temperature, ambient density, and injection pressure, Combustion and Flame, vol. 138, pp. 114-135, 2004.

[22] E. Mancaruso, S.S. Merola, B.M. Vaglieco, Study of the multi-injection combustion process in a transparent direct injection common rail diesel engine by means of optical techniques, Int. J. Engine Res. Vol 9, issue 6, pp. 483-498, 2008.

[23] D.F. Kronholm, J.B. Howard, Analysis of soot surface growth pathways using published plug-flow reactor data with new particle size distribution measurements and published premixed flame data, Proceedings of the Combustion Institute, vol. 28, pp. 2555-2561, 2000.

[24] J.M. Desantes, J. Arrègle, J.J. López, A. Cronhjort, Scaling laws for free turbulent gas jets and diesel-like sprays, Atomization and Sprays, vol. 16, pp. 443-473, 2006.

[25] F. Payri, J.V. Pastor, J.M. García, J.M. Pastor, Contribution to the application of two-colour imaging to diesel combustion, Measurement Science and Technology, vol. 18, pp. 2579-2598, 2007.

[26] J. Dec, A Conceptual Model of DI Diesel Combustion Based on Laser-Sheet Imaging, SAE Technical Paper 970873, 1997.